

LARGE-SCALE VORTICAL MOTION AND COMBUSTION NOISE CONTROL IN SWIRL-STABILIZED COMBUSTOR

M. Shimura, M. Tanahashi and T. Miyauchi

Department of Mechanical and Aerospace Engineering,
Tokyo Institute of Technology
2-12-1 Ookayama, Meguro-ku, Tokyo 152-8550, Japan
mshimura@navier.mes.titech.ac.jp

G.-M. Choi

School of Mechanical Engineering, College of Engineering,
Pusan National University
Busan 609-735, Korea
choigm@pusan.ac.kr

ABSTRACT

To clarify the mechanisms of combustion oscillation, combustion noise and their suppression by secondary fuel injection, simultaneous measurements of stereoscopic particle image velocimetry (SPIV) and pressure fluctuation in combustion chamber were conducted on several planes of a swirl-stabilized turbulent premixed flame for no control case and noise-controlled case by continuous secondary fuel injection. Velocities measured by SPIV were averaged in 8 phases of the pressure fluctuation and streamlines were obtained from the phase-averaged velocities. For no control case, large-scale vortical structures are generated in regions around the axial centerline of the combustor and outer edge of the swirl injector in the phase of low pressure. With increasing pressure, they move near the contour surface of mean progress variable $\bar{c} = 0.5$ which have been obtained in the previous study. This large-scale vortical motion induces fluctuation of flame front and enhances entropy term in the acoustic sound source. The secondary fuel injection suppresses the velocity fluctuation in the inner recirculation zone, resulting in reduction of combustion noise. These results show that control of the large-scale vortical motion is important for reduction of combustion noise.

INTRODUCTION

Lean premixed combustion which is a candidate for high efficiency and low emission gas turbines is prone to combustion oscillations. Rayleigh (1878) showed that combustion oscillations are mainly caused by the feedback interaction between natural acoustic modes of the combustor and oscillation of heat release rate. Sound generation mechanisms in turbulent reactive flows, which are closely related to combustion instabilities, have been investigated by direct numerical simulations (Li et al. 2000; Zhao and Frankel 2001; Tanahashi et al. 2002). In general, acoustic sound source can be decomposed into Reynolds stress, entropy and viscous terms. It is well-known that the entropy term is a main sound source in combustion field and is dominated by fluctuation of heat release rate. However, the entropy term from turbulent energy dissipation rate is also important (Tanahashi et al. 2002; Choi et al. 2003). The distribution of entropy term is determined by energy dissipation rate in the area where the heat release rate is very small. Fine scale

eddies are closely related to the entropy term, because turbulent energy dissipation rate is very high around fine scale eddies (Tanahashi et al. 2001; Tanahashi et al. 2004). The fine scale eddies are also closely related with the Reynolds stress term (Choi et al. 2003). Therefore, fine scale eddies of turbulence are important sound sources in three-dimensional turbulent flows. These facts suggest that the key point to develop a control scheme of combustion noise is how to suppress the fluctuations of heat release rate and how to control the fine scale eddies of turbulence.

Combustion control by secondary fuel injection has been studied by many researchers (Dowling and Morgans 2005). Hong et al. (2002) have conducted experiments to evaluate the control law under the wide-range operation of a generic combustor using secondary fuel injection. Lee et al. (2000) have investigated effects of secondary fuel injection location on the effectiveness of active combustion control in a laboratory-scale dump combustor at atmospheric pressure. In the previous study (Choi et al. 2005), we have revealed that, due to the modification of local flame structure by secondary fuel injection, combustion noise and NO_x emission can be reduced simultaneously.

However, to achieve more effective control of oscillating combustion, it is necessary to get detailed information about flame structure and turbulent structure in stable and unstable conditions of combustor. 3D flame structures of turbulent premixed flames have been investigated by OH planar laser induced fluorescence (PLIF) in our previous study (Tanahashi et al. 2008). It was revealed that the secondary fuel injection reduces fluctuation of flame front in flame zone and that of high temperature gas in recirculation zone. Dawson et al. (2005) investigated the destabilizing effect of combustion instability on the shape and size of recirculation zones by measuring velocity field with a laser doppler velocimetry (LDV) and pressure. Weigand et al. (2006) conducted LDV, PLIF of OH and CH, and laser Raman scattering in swirling methane-air lean diffusion flames to understand the physical and chemical processes leading to the different behavior of the flames. Armitage et al. (2006) investigated acoustically forced lean premixed turbulent bluff-body stabilized flames by using CFD of turbulent combustion and comparing that with their experimental work (Balachandran et al. 2005).

The objectives of this study are to investigate the relation

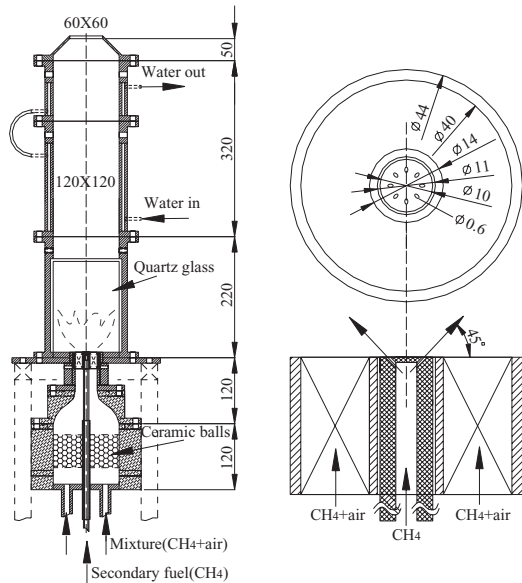


Figure 1: Schematic of swirl-stabilized combustor and details of swirl vanes and secondary fuel injection nozzle.

between the large-scale vortical motion and pressure fluctuation in a noise-controlled swirl-stabilized combustor, and to reveal the mechanisms of combustion oscillation, combustion noise and their suppression by secondary fuel injection. In this study, simultaneous measurements of SPIV and pressure fluctuation in combustion chamber were conducted on several planes of the combustor, and large vortical structures were extracted by the phase-averaged velocity maps. Obtained results are discussed with the 3D flame structures obtained in the previous study (Tanahashi et al. 2008).

EXPERIMENTAL APPARATUS

The swirl-stabilized combustor which has been investigated in our previous works (Choi et al. 2005; Tanahashi et al. 2008) is used. Figure 1 shows the schematic of the swirl-stabilized combustor and details of secondary fuel injection nozzle. This combustion rig consists of a contraction section, a swirl nozzle section and a combustion chamber. The swirl nozzle of 40 mm outer diameter is mounted on the contraction section. The inner cross-section of the combustion chamber is 120 mm x 120 mm, and the outlet of combustion chamber is contracted to 60 mm x 60 mm. The total length of the chamber is 590 mm. On each side of combustion chamber, a silica glass plate of 120 mm x 170 mm and 5 mm thickness is installed to allow optical access. Combustion chamber upper than 220 mm is cooled by water. The swirl nozzle has 8 swirl vanes of 14 mm inner diameter and 40 mm outer diameter, inclined 45° from the nozzle axis. Methane-air premixed gas, which is not heated, passes through the swirl vanes and the flame was stabilized at the swirl vanes. The secondary fuel nozzle is mounted at the hub of the swirler and has 8 injection holes (ID = 0.6 mm) inclined at 45° to the mainstream direction. The secondary fuel injection can be modulated by a valve (MAC VALVES, 34BABA-GEME-1BA). In this study, the valve is driven by direct voltage (24 V) and is always open for continuous secondary fuel injection.

SPIV AND PRESSURE FLUCTUATION MEASUREMENT

Figure 2 shows a schematic of SPIV system. The sys-

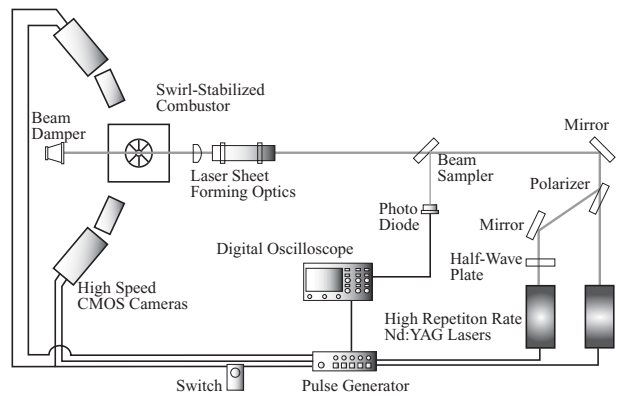


Figure 2: Schematic diagram of SPIV system.

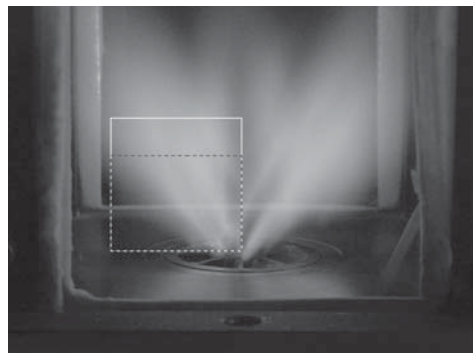


Figure 3: Long-time exposure photo of methane-air turbulent premixed flame controlled by continuous secondary fuel injection. Gray dotted and white boxes: measurement regions including centerline of the combustor for no control and continuous injection cases.

tem consists of two high-repetition Nd-YAG Lasers (Lee Laser, LDP-100MQG), several optics, two high-speed CMOS cameras (Vision Research, Phantom V7.1, 800 x 600 pixels) and a pulse/delay generator (Labsmith, LC880). Two laser beams become doubled-pulsed through the laser beam combining optics which include a half-wave plate and a polarizer. Time interval (Δt) of double-pulsed beams is confirmed by a photo diode and a digital oscilloscope. The laser beams were expanded by the laser sheet forming optics, and were scattered by 2 μm SiO₂ particles mixed in the methane-air premixed gas. Scattered light is detected by the CMOS cameras with telephotographic lens (Nikon, Micro-nikkor 200 mm/f4). The CMOS cameras are located with 19° inclined forward with respect to normal to the measurement plane to capture forward scattered light. In order to obtain particle images in good focus over the whole measurement region, the Scheimpflug condition (Prasad 1995) was used.

Pressure transducer (JTEKT, PD104) with a water-cooling connection tube was attached to the combustion chamber at 500 mm downstream from the exit of swirl injector. Pressure signal, a start signal of measurement and strobe signal of CMOS camera were simultaneously recorded by PC with A/D converter (National Instruments, PCI-6115). Sampling rate was set to 200 kHz to detect strobe signal which is shorter than 10 μsec .

EXPERIMENTAL CONDITIONS

Measurements were conducted for the condition without secondary fuel injection, which is referred as no control case, and for the noise-controlled condition with continuous

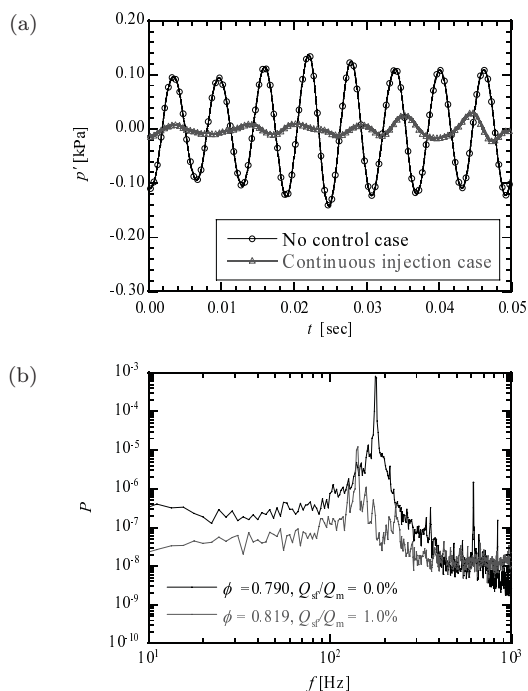


Figure 4: Characteristics of pressure fluctuation in the combustor for no control and continuous injection cases. (a) An example of time series data (≤ 500 Hz). (b) Power spectra.

secondary fuel injection, which is called continuous injection case hereafter. The flow rate of the main methane-air mixture (Q_m) was selected to 300 L/min for both cases. Equivalence ratio (ϕ) of main mixture was set to 0.790 for no control case. As for the case of continuous injection, equivalence ratio (ϕ) of main mixture was 0.717 and flow rate of the secondary fuel injection (Q_{sf}) was set to 1% of Q_m (total $\phi = 0.819$).

Figure 3 shows measurement regions of SPIV on a long-time exposure photo of methane-air premixed flame with continuous secondary fuel injection. The x , y and z axes of coordinates in measurement region are set to main stream direction of the combustor, laser travel direction and normal direction to the other axes, respectively, and origin of the coordinate system is set to the center of swirler exit. Gray dotted box in Fig. 3 corresponds to a whole measurement region including centerline of the combustor for no control case. The size of the box is 27.0 mm \times 37.2 mm and central position of the box is (15.5 mm, 18.6 mm, 0 mm). The measurement region was divided into four rectangles which overlap 2.5 mm each other, and SPIV measurements were conducted on each area in order to improve spatial resolution of SPIV. White box in Fig. 3 corresponds to a measurement region for continuous injection case. The size of this box is 39.2 mm \times 37.2 mm and central position of the measurement region is (21.6 mm, 18.6 mm, 0 mm). The measurement region was divided into six rectangles on which SPIV measurements were conducted. Flame zone for continuous injection case was pushed downstream by secondary fuel injection (Tanahashi et al. 2008). These measurement regions covered recirculation zone and flame zone, and were moved from the plane including the centerline of the combustor to the edge of the combustor with the distance of 4 mm. Total number of the measurement planes is 5 in one side of the combustor for no control case ($z = 0 \sim 16$ mm). As for continuous injection case, SPIV was conducted on

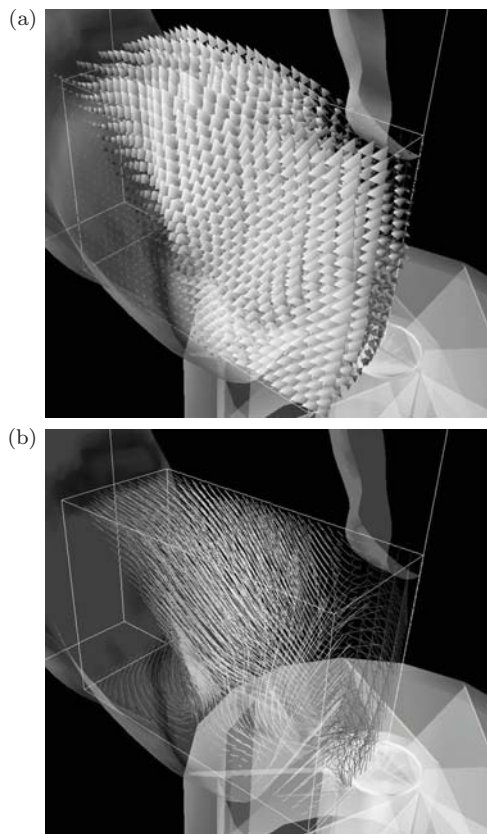


Figure 5: Mean velocity map (a) and streamlines (b) obtained from the mean velocity for no control case. Gray surfaces correspond to $\bar{c} = 0.5$ obtained in the previous study (Tanahashi et al. 2008).

the planes of $z = 0$ mm and 16 mm. Spatial resolution of SPIV was 1.23 mm, and Δt was altered in accordance with turbulence and turbulent combustion characteristics of measurement region (15 \sim 30 μ sec).

PRESSURE FLUCTUATION IN THE SWIRL-STABILIZED COMBUSTOR

The characteristics of pressure fluctuation in the combustor are shown in Fig. 4. Figure 4 (a) shows an example of time-series pressure fluctuation for no control and continuous injection case. Pressure signal is filtered by low-pass filter of 500 Hz. The pressure fluctuation is suppressed by continuous secondary fuel injection drastically. Figure 4 (b) shows power spectra obtained from raw pressure data up to 1 kHz. Peak frequency of the pressure fluctuation changes from 178 Hz to 142 Hz, and energy at the peak frequency decreases significantly for continuous injection case. However, new peaks are induced at about 128 Hz and 157 Hz. These results indicate that continuous secondary fuel injection does not sufficiently suppress combustion oscillation and that alternative feedback interaction is induced by secondary fuel injection. This alternative feedback interaction can be eradicated by controlling injection frequency of the secondary fuel injection (Tanahashi et al. 2008). In this study, velocities obtained by SPIV were averaged in 8 phases of the pressure fluctuation. Here, the phase of SPIV data was estimated by finding local extrema of filtered pressure data (≤ 500 Hz) and the velocity data is separated into 8 phase bins (denoted by Δ).

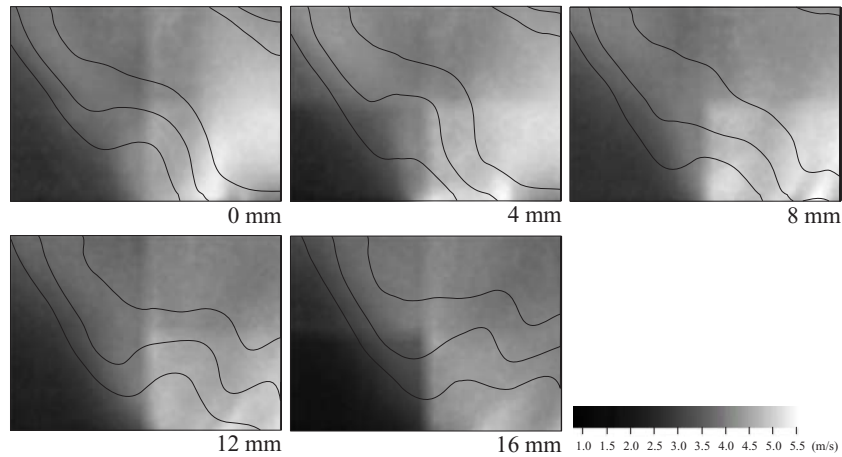


Figure 6: Turbulent intensity on each measurement plane for no control case. Solid lines in each plane represents iso-lines of mean progress variable $\bar{c} = 0.3, 0.5$ and 0.7 from beneath.

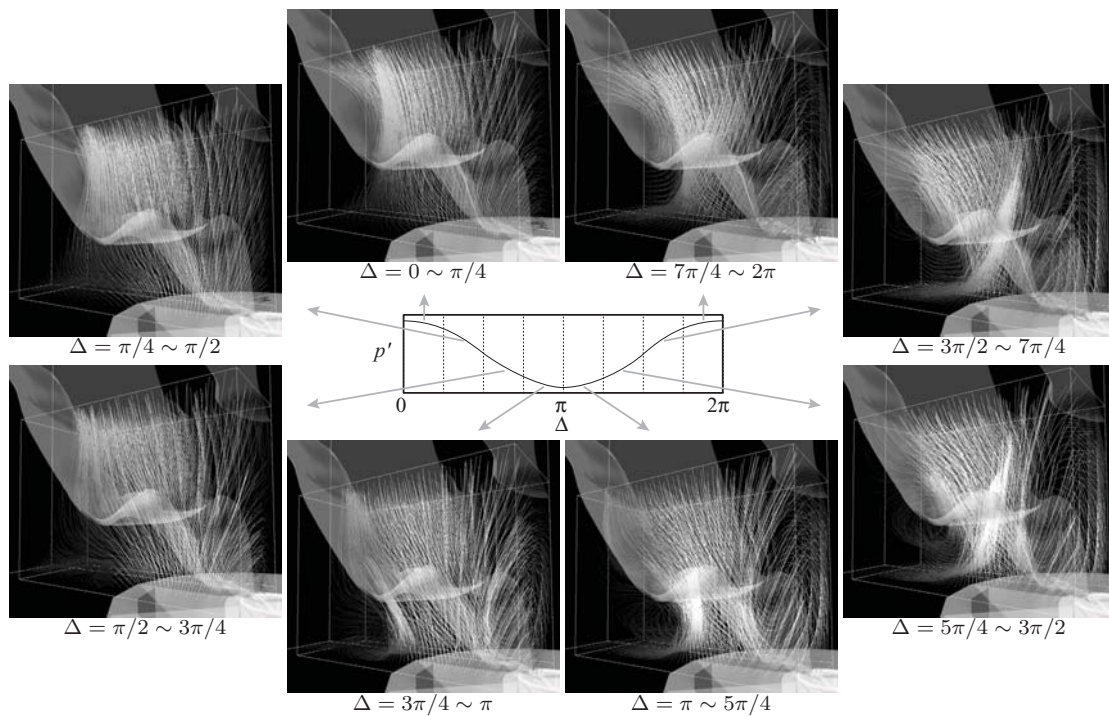


Figure 7: Distributions of streamlines obtained from the phase-averaged velocity with the contour surface of mean progress variable $\bar{c} = 0.5$ obtained in the previous study (Tanahashi et al. 2008).

LARGE-SCALE VORTICAL MOTIONS IN THE SWIRL-STABILIZED COMBUSTOR

Instantaneous velocity map was calculated by 2-step hierarchical method (Kumar and Banerjee 1998) and a window-offset method (Westerweel et al. 1997). Overlap of interrogation regions was set to 80%. From two-dimensional velocity fields obtained by each CMOS camera, three-component velocity vectors on a two-dimensional plane were calculated by using a geometrical relation (Willert, 1997; Prasad, 2000). Figure 5 shows mean velocity map and streamlines obtained from the mean velocity for no control case. White surface in Fig. 5 represents contour surface of mean progress variable $\bar{c} = 0.5$ obtained in the previous OH PLIF measurement (Tanahashi et al. 2008). Mean velocity was obtained from 2,400 instantaneous velocity maps.

The largest vector represents maximum velocity of 11.5 m/s. Although velocity of fluid increases through flame surface, there are low velocity regions which indicates existence of shear layers due to the swirl injector. Inner and outer recirculation zones are formed near the axial centerline of the combustor and near the wall of combustion chamber, respectively.

Figure 6 shows rms of velocity fluctuation (u_{rms}) on different measurement plane in the z direction for no control case. Black solid lines in Fig. 6 represents iso-lines of mean progress variable $\bar{c} = 0.3, 0.5$ and 0.7 from beneath. Turbulent intensity near exit of the swirl injector shows high value on the plane of $z = 0, 4$ and 8 mm. These high turbulent intensity regions overlap with flame brush. Furthermore, turbulent intensity shows high value in the inner recircula-

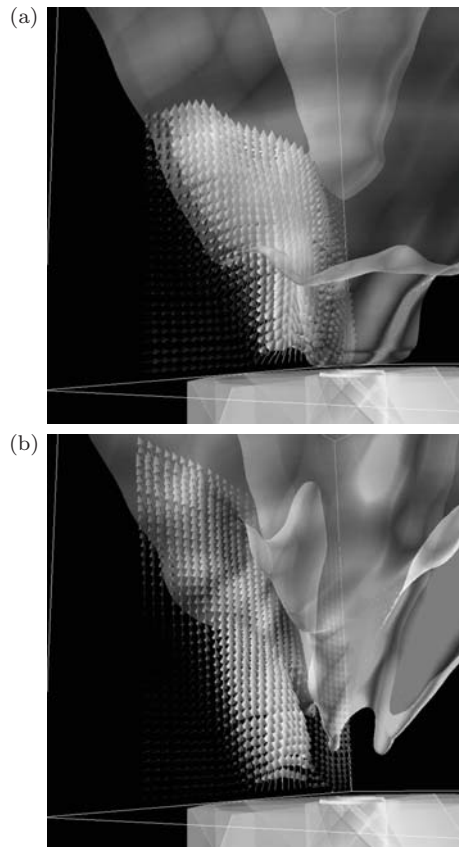


Figure 8: Mean velocity map on the measurement planes of $z = 0$ mm for no control case (a) and continuous injection case (b). White surfaces correspond to $\bar{c} = 0.5$ which have been obtained in the previous study (Tanahashi et al. 2008).

tion zone on the plane of $z = 0$ and 4 mm, which denotes that recirculating high temperature gas fluctuates considerably in space and time. These turbulent fluctuations induce fluctuation of flame front and resultant pressure fluctuation in the combustor.

Figure 7 shows streamlines obtained from the phase-averaged velocity maps with the contour surface of mean progress variable $\bar{c} = 0.5$ reported in the previous study (Tanahashi et al. 2008). Since the mean progress variable is not phase-averaged one, same contour surface is shown in all phases. The averaged velocity in each phase was obtained from about 300 instantaneous velocity maps. In the phase of high pressure ($\Delta = 0 \sim \pi/4$ in Fig. 7), velocity in burnt region is high, and inlet velocity is relatively low. In these phases, the size of inner recirculation zone near the hub is relatively small. The inlet velocity increases with the decrease of pressure in the combustor. Large-scale vortical structures are formed in regions around the axial centerline of the combustor and outer edge of the swirl injector ($\Delta = \pi/4 \sim 3\pi/4$ in Fig. 7). In the phase of the lowest pressure ($\Delta = 3\pi/4 \sim 5\pi/4$ in Fig. 7), the large-scale vortical structures develop and move downstream, which raises pressure in the combustor. In the phase of $\Delta = 5\pi/4 \sim 2\pi$ in Fig. 7, the inlet velocity decreases with the increase of pressure in the combustor and the vortical structures move and fade away downstream. Since the vortical structures are moving near the contour surface of $\bar{c} = 0.5$, they induce the fluctuation of flame front and enhance entropy term of the acoustic sound source. The results obtained in this section

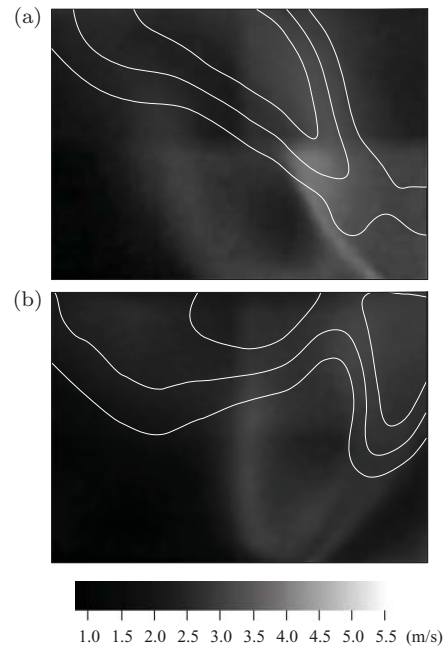


Figure 9: Distributions of turbulent intensity on the measurement plane of $z = 0$ mm (a) and 16 mm (b) for continuous injection case. Solid lines in each plane represents iso-lines of $\bar{c} = 0.3, 0.5$ and 0.7 from beneath.

suggest that suppression of the large-scale vortical motion formed in the recirculation zones is important for the reduction of flame front fluctuation and combustion noise.

SUPPRESSION OF LARGE-SCALE VORTICAL MOTION BY SECONDARY FUEL INJECTION

Figure 8 shows mean velocity map on the measurement planes of $z = 0$ mm for no control and continuous injection cases with contour surface of $\bar{c} = 0.5$. Region of $\bar{c} = 0.5$ spreads outwards and is pushed up by the jets of the secondary fuel for continuous injection case. No flame regions intrude into the downstream and concave structures are formed (Tanahashi et al. 2008). Compared with no control case, the region of recirculation zone for continuous injection case is expanded, and magnitude of fluid velocity on the plane of $z = 0$ is decreased in near swirler exit.

Figure 9 shows distribution of turbulent intensity on the measurement planes of $z = 0$ mm and 16 mm for continuous injection case. Solid lines in each plane represents iso-lines of mean progress variable $\bar{c} = 0.3, 0.5$ and 0.7 from beneath. Figure 9 (a) shows that continuous secondary fuel injection suppresses the turbulent intensity around the inner recirculation zone and near the exit of swirl injector compared with no control case shown in Fig. 6. However, turbulent intensity in a region near the secondary fuel injection hole is higher than the surroundings. This fluctuation induces alternative instability mode of the combustor shown in the pressure spectra (Fig. 4 (b)). In Fig. 9 (b), turbulent intensity is relatively low in the upstream of concave structure. By adding secondary fuel continuously, turbulent intensity was reduced to approximately half of no control case over all measurement regions. In the previous study (Choi et al. 2005), it has been revealed that noise is reduced about 15 dB by continuous secondary fuel injection compared with that generated in the similar equivalence ratio without secondary fuel injection ($\phi = 0.790$). The secondary fuel injection sup-

presses flame front fluctuation and resultant fluctuation of heat release rate by reducing the velocity fluctuations. This suppression contributes to reduction of the entropy term in the acoustic sound sources. Furthermore, suppression of inlet velocity fluctuation corresponds to reduction of fine scale eddies and decreases Reynolds stress term induced by turbulent motion and the entropy term due to energy dissipation rate.

CONCLUSIONS

To investigate the mechanisms of combustion oscillation, combustion noise and their suppression by secondary fuel injection, simultaneous measurements of SPIV and pressure fluctuation were conducted on multiple planes of methane-air turbulent premixed flames in the swirl-stabilized combustor for no control and continuous secondary fuel injection cases. Velocities measured by SPIV were averaged in 8 phases of the pressure fluctuation and streamlines were obtained from the phase-averaged velocity maps.

For no control case, large-scale vortical structures are generated in regions around the axial centerline of the combustor and outer edge of the swirl injector in the pressure decreasing phase. The vortical structures develop with moving downstream in the phase of the lowest pressure. They move near the contour surface of mean progress variable $\bar{c} = 0.5$ in the pressure increasing phase, and fade away downstream in the phase of high pressure. This vortical motion induces flame front fluctuation, i.e. fluctuation of heat release rate, and enhances entropy terms in the acoustic sound source. Therefore, suppression of the large-scale vortical motion is important for reduction of combustion noise.

The secondary fuel injection suppresses the velocity fluctuation around the inner recirculation zone and that near the exit of swirl injector. These suppressions cause reduction of flame front fluctuation and fluctuation of heat release rate. Therefore, secondary fuel injection contributes to reduction of the entropy term in the acoustic sound sources. Furthermore, suppression of inlet velocity fluctuation by the secondary fuel corresponds to reduction of fine scale eddies and decreases Reynolds stress term caused by turbulent motion and entropy term due to energy dissipation rate.

ACKNOWLEDGMENTS

This work is partially supported by Grant-in-Aid for Young Scientists (S) (No. 20676004) of Japan Society for the Promotion of Science and M. Shimura is supported by Grant-in-Aid for JSPS Fellows (No. 19 · 10540) of Japan Society for the Promotion of Science.

REFERENCES

Armitage, C. A., Balachandran, R., Mastorakos, E., and Cant, R. S., 2006, "Investigation of the Nonlinear Response of Turbulent Premixed Flames to Imposed Inlet Velocity Oscillations", *Combustion and Flame*, Vol. 146, pp. 419-436.

Balachandran, R., Ayoola, B. O., Kaminski, C. F., Dowling, A. P., and Mastorakos, E., 2005, "Experimental Investigation of the Nonlinear Response of Turbulent Premixed Flames to Imposed Inlet Velocity Oscillations", *Combustion and Flame* Vol. 143, pp. 37-55.

Choi, G.-M., Li, Y., Tanahashi, M., and Miyauchi, T., 2003, "Sound Generation Mechanism in Turbulent Mixing Layer", *Turbulent Shear Flow Phenomena*, Vol. 3, No. 2, pp. 729-734.

Choi, G.-M., Tanahashi, M., and Miyauchi, T., 2005,

"Control of Oscillating Combustion and Noise Based on Local Flame Structure", *Proceedings of the Combustion Institute*, Vol. 30, No. 2, pp. 1807-1814.

Dawson, J. R., Rodriguez-Martinez, V. M., Syred, N., and O' Doherty, T., 2005, "The Effect of Combustion Instability on the Structure of Recirculation Zones in Confined Swirling Flames", *Combustion Science and Technology*, Vol. 177, pp. 2349-2371.

Dowling, A. P., and Morgans, A. S., 2005, "Feedback Control of Combustion Oscillations", *Annual Review of Fluid Mechanics*, Vol. 37, pp. 151-182.

Hong, B.-S., Ray, A., and Yang, V., 2002, "Wide-Range Robust Control of Combustion Instability", *Combustion and Flame*, Vol. 128, No. 3, pp. 242-258.

Kumar, S., and Banerjee, S., 1998, "Development and Application of a Hierarchical System for Digital Particle Image Velocimetry to Free-Surface Turbulence", *Physics of Fluids*, Vol. 10, pp. 160-177.

Lee, J. G., Kim, K., and Santavicca, D. A., 2000, "Effect of Injection Location on the Effectiveness of an Active Control System Using Secondary Fuel Injection", *Proceedings of the Combustion Institute*, Vol. 28, No. 1, pp. 739-746.

Li, Y., Tanahashi, M., and Miyauchi, T., 2000, "Sound Generation in Chemically Reacting Mixing Layers", *Transactions of the Japan Society of Mechanical Engineers B*, Vol. 66, No. 648, pp. 2117-2124.

Prasad, A. K., 1995, "Scheimpflug Stereocamera for Particle Image Velocimetry in Liquid Flows", *Applied Optics*, Vol. 34, No. 30, pp. 7092-7099.

Prasad, A. K., 2000, "Stereoscopic Particle Image Velocimetry", *Experiments in Fluids*, Vol. 29, pp. 103-116.

Rayleigh, L., 1878 (reedited in 1945), "The Theory of Sound", New York, Dover.

Tanahashi, M., Iwase, S., and Miyauchi, T., 2001, "Appearance and Alignment with Strain Rate of Coherent Fine Scale Eddies in Turbulent Mixing Layer", *Journal of Turbulence*, Vol. 2, No. 6.

Tanahashi, M., Tsukinari, S., Saitoh, T., Miyauchi, T., Choi, G.-M., Ikame, M., Kishi, T., Harumi, K., and Hiraoka, K., 2002, "On the Sound Generation and its Controls in Turbulent Combustion Field", *Proceedings of 3rd Symposium on Smart Control of Turbulence*, pp. 149-160.

Tanahashi, M., Kang, S. J., Miyamoto, T., Shiokawa, S., and Miyauchi, T., 2004, "Scaling Law of Fine Scale Eddies in Turbulent Channel Flows up to $Re_\tau = 800$ ", *International Journal of Heat and Fluid Flow*, Vol. 25, pp. 331-340.

Tanahashi, M., Inoue, S., Shimura, M., Taka, S., Choi, G.-M., and Miyauchi, T., 2008, "Reconstructed 3D Flame Structures in Noise-Controlled Swirl-Stabilized Combustor", *Experiments in Fluids*, Vol. 45, No. 3, pp. 447-460.

Weigand, P., Meier, W., Duan, X. R., Stricker, W., and Aigner, M., 2006, "Investigations of Swirl Flames in a Gas Turbine Model Combustor: I. Flow Field, Structures, Temperature, and Species Distributions", *Combustion and Flame*, Vol. 144, pp. 205-224.

Westerweel, J., Dabiri, D., and Garib, M., 1997, "The Effect of a Discrete Window Offset on the Accuracy of Cross-Correlation Analysis of Digital PIV Recordings", *Experiments in Fluids*, Vol. 23, pp. 20-28.

Willert, C., 1997, "Stereoscopic Digital Particle Image Velocimetry for Application in Wind Tunnel Flows", *Measurement Science and Technology*, Vol. 8, pp. 1465-1479.

Zhao, W., and Frankel, S. H., 2001, "Numerical Simulations of Sound Radiated from an Axisymmetric Premixed Reacting Jet", *Physics of Fluids*, Vol. 13, No. 9, pp. 2671-2681.